

Disordered, Strongly Scattering Porous Materials as Miniature Multipass Gas Cells

Tomas Svensson,^{1,*} Erik Adolphsson,² Märta Lewander,¹ Can T. Xu,¹ and Sune Svanberg¹

¹*Department of Physics, Lund University, Box 118, SE-221 00 Lund, Sweden*

²*Ceramic Materials, SWEREA IVF, Box 104, SE-431 22 Mölndal, Sweden*

(Received 31 January 2011; revised manuscript received 16 June 2011; published 27 September 2011)

We investigate the interaction of light and gas in strongly scattering nano- and macroporous media. Manufacturing and structural characterization of ZrO_2 , Al_2O_3 and TiO_2 ceramics with different pore sizes, measurements of optical properties using photon time-of-flight spectroscopy, and high-resolution laser spectroscopy of O_2 at 760 nm are reported. We show that extreme light scattering can be utilized to realize miniature spectroscopic gas cells. Path length enhancement factors up to 750 are reached (5.4 m path through gas for light transmitted through a 7 mm ZrO_2 with 49% porosity and 115 nm pores).

DOI: 10.1103/PhysRevLett.107.143901

PACS numbers: 42.25.Dd, 07.07.Df, 42.62.Fi, 78.67.Rb

Strongly scattering media have received an enormous amount of attention for many years, yet new fascinating aspects are continuously reported. In addition to constituting the physical system for fundamental investigation of Anderson localization of light [1,2] and random lasing [3,4], strong turbidity can also be used for, e.g., light trapping in solar cells [5] and focusing beyond the diffraction limit [6]. Here, we merge this tradition with the field of high-resolution laser spectroscopy, reporting on the exciting physics of light-gas interaction in strongly scattering porous media. Not only do we find this a topic rich in unexplored physics, but it could also have an impact on the rapidly advancing and already commercially successful field of spectroscopic gas sensing. Throughout the years, this field has directed massive efforts towards improving detection limits by achieving long interaction path lengths. Prominent examples include the use of conventional multipass gas cells [7,8], sophisticated high-finesse cavities [9–12], gas-filled holey fibers [13–15], integrating spheres [16,17], and diffusive reflectors [18]. Despite this rich flora of approaches, there is a continuous struggle to reduce size, gas volume, cost and alignment complexity [19–21]. In the present work, we describe how extreme light scattering in disordered porous materials can be used to realize miniature gas cells. Near-infrared light diffusively transmitted through a few millimeters of highly porous sintered ceramics is shown to have traveled up to several meters through gas. This essentially different approach to path length enhancement opens a new route to compact, alignment-free and low-cost optical sensor systems. At the same time, the markedly enhanced gas absorption imprints reported here may constitute a new experimental basis for studies of light propagation in strongly scattering media. Gas absorption is a direct way of measuring how light samples complex porous media, and may be useful in studies of, e.g., the complex multiple scattering occurring in densely packed particle systems.

Multiple scattering always forces photon path lengths to greatly exceed physical source-detector separation (Fig. 1),

and this multipass effect will in the case of porous media result in enhanced gas absorption imprints. As shown in previous work on spectroscopy of gases in porous media [22], absorption related to the solid is easily distinguished from gas phase absorption due to the great difference in spectral sharpness. Here, by utilizing disordered and highly porous materials based on low-absorption ceramic materials such as alumina (Al_2O_3 , refractive index $n = 1.76$ at 760 nm), zirconia (ZrO_2 , $n = 2.14$) and titania (TiO_2 , $n = 2.49$), we report on remarkable path length enhancements. The strong scattering of nanoporous alumina and its possible application to spectroscopic gas sensing, was brought to attention in recent work on spectroscopy of confined gases and wall collision line broadening [23]. Manufacturing and use of high refractive index materials with much higher scattering efficiency, as presented here, results in remarkable path length enhancements and thus also dramatically improve the gas cell potential.

We have manufactured and studied five different porous sintered ceramic materials; one titania, two alumina, and two zirconia materials. The pore structure has been investigated using mercury intrusion porosimetry [24], and all

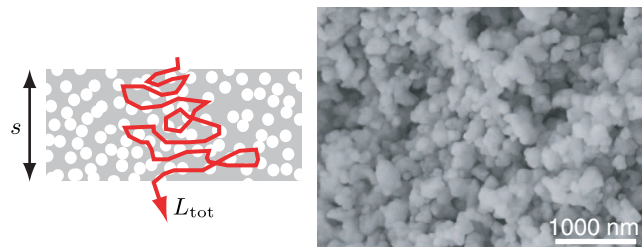


FIG. 1 (color online). Illustration of porous media as gas cells (left), and a scanning electron microscope image of a utilized nanoporous zirconia with 115 nm pores (right). When light propagates through a strongly scattering and porous material of thickness s , the average path length of transmitted light (L_{tot}) will greatly exceed s . The path length through gas (L) is approximately proportional to L_{tot} and the porosity ϕ . The enhancement of the gas interaction path length may be defined as $N = L/s$.

materials have narrow, well defined pore size distributions. The titania was manufactured by sintering of Kronos 1001 powder (Kronos, Germany) for 2 hours at 900° C, and is nanoporous with a 42% porosity and pores in the 79 ± 10 nm range (width here defined as the half width at half max, HWHM, of the pore size distribution). One alumina is nanoporous with 69 ± 8 nm pores and a 35% porosity and was made by sintering AKP30 (Sumitomo, Japan) for 10 min at 1000° C. The second alumina is macroporous with $3.7 \pm 0.4 \mu\text{m}$ pores and a 34% porosity and was manufactured to 92.5% from AA10 (Sumitomo, Japan), the rest being a 40 nm silica powder used as a binder (sintering for 45 min at 1400° C). The zirconia materials are nanoporous and both have a 49% porosity, pores being 43 ± 6 nm and 115 ± 15 nm, respectively, (sintering for 2 h at 900° C using the TZ3YBE and TZ3YSBE powders from Tosho, Japan). It should be noted that ceramics sintering is a highly reproducible procedure, and that the optical characteristics discussed in this work typically vary only a few percent between sample replicas.

The scattering and absorption of these materials have been measured in the 700–1400 nm range by employing photon time-of-flight spectroscopy (PTOFS) [25]. Short (ps) light pulses are injected into the samples and the temporally broadened transmitted pulses are detected and resolved in time. Evaluation is based on diffusion theory and involves fitting of absorption (μ_a) and reduced scattering coefficients (μ'_s) [26]. In fact, PTOFS provides information on the diffusion coefficient, and a volume-averaged refractive index is used to estimate transport velocity and then reach μ'_s (the refractive index of the solid, for each wavelength, is based on a Sellmeier equation). Given the highly irregular structure of sintered ceramics, our disregard of potential reduction of transport velocity due to resonant scattering [27] should be justified. Furthermore, since effective medium theories for strongly scattering materials are not fully developed [28–30], we use volume averaging as a convenient approximation. The measured μ'_s are presented in Fig. 2(a), revealing a strong dependence on refractive index and pore size. The independence of derived coefficients on sample geometry has been verified by performing measurements where the radial source and detector separation is varied (effectively probing different propagation distances). The scattering of the two strongest scatterers even approach that of the materials used in the quest for Anderson localization of light [1,2]. At 700 nm, the transport mean free paths of photons ($l_t = 1/\mu'_s$) are about $0.7 \mu\text{m}$ and $1.0 \mu\text{m}$ for the titania and 115 nm zirconia, respectively, (the shortest photon mean free path observed, published in connection with work on Anderson localization, is about $0.2 \mu\text{m}$ [1]). It is also interesting to note that the materials with pore size smaller than the wavelength exhibit a λ^{-4} Rayleigh-type scattering dependency. The 43 nm zirconia is an exception, and its slower wavelength dependence indicates that

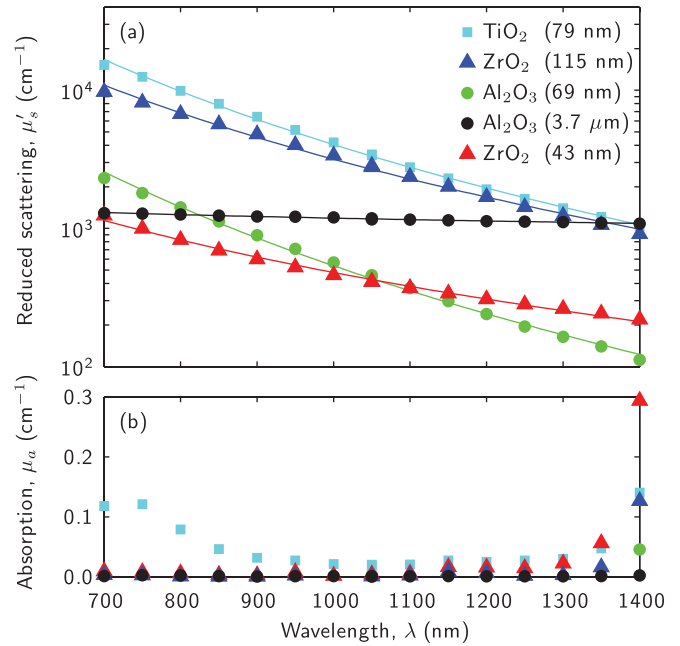


FIG. 2 (color). Optical properties of the ceramic materials. Reduced scattering coefficients are shown in (a), and absorption coefficients in (b). Solid lines in (a) show fitted $a \times (\lambda/\mu\text{m})^{-b}$ curves and give information on scattering decay, being $4045 \times \lambda^{-4.0}$ for the titania, $537 \times \lambda^{-4.4}$ and $1187 \times \lambda^{-0.3}$ for the aluminas, and $3167 \times \lambda^{-3.5}$ and $480 \times \lambda^{-2.4}$ for the zirconias, respectively.

collective heterogeneity dominates over the weak scattering of individual pores. The macroporous alumina, on the other hand, shows that a heterogeneity larger than the wavelength can be used to maintain high scattering over a large spectral range.

The estimated absorption of the materials is shown in Fig. 2(b). As expected for these ceramic materials, the absorption is low in the near-infrared range. The titania, however, exhibit a fairly strong absorption in the short wavelength region, being a tail of strong ultraviolet absorption. All materials, except the macroporous alumina, exhibit significant absorption at 1400 nm related to adsorbed water.

Light-gas interaction in the porous ceramics is investigated using high-resolution near-infrared tunable diode laser absorption spectroscopy (TDLAS) of molecular oxygen. The utilized instrument is described in detail in Ref. [31]. Briefly, light from a 0.3 mW VCSEL diode laser is injected into the pillbox-shaped ceramic samples, and diffuse transmission is detected by a $5.6 \times 5.6 \text{ mm}^2$ large-area photodiode (no alignment needed). The laser is tuned over the R9Q10 absorption line at 760.654 nm, which at atmospheric conditions has a peak absorption coefficient of $2.7 \times 10^{-4} \text{ cm}^{-1}$ and a linewidth of $\Gamma = 1.6 \text{ GHz}$ (HWHM). Optical interference noise, an important limitation in laser spectroscopy of gases in turbid porous media, is suppressed by means of laser beam dithering [32].

TABLE I. Results from near-infrared (760.654 nm) spectroscopy of molecular oxygen in sintered ceramic materials. The table states material thickness (s), photon transport mean free path at 760 nm (l_t), porosity (ϕ), pore size (d), detected transmission (T), spectroscopic linewidth (Γ), path length through gas (L), and path length enhancement ($N = L/s$). Sample diameters were in all cases 12–14 mm.

Material	s (mm)	l_t (μm)	ϕ (%)	d (nm)	T (%)	Γ (GHz)	L (cm)	$N = L/s$ (-)
ZrO ₂	7.2	1.3	48.8	115 \pm 15	0.003	2.218 \pm 0.009	541 \pm 4	\approx 750
Al ₂ O ₃	5.5	5.8	34.5	69 \pm 8	0.02	2.36 \pm 0.02	83.3 \pm 0.8	\approx 150
TiO ₂	1.4	0.8	42.4	79 \pm 10	0.001	2.17 \pm 0.09	19 \pm 2	\approx 135
ZrO ₂	7.0	10.4	48.6	43 \pm 6	0.05	2.75 \pm 0.06	86 \pm 4	\approx 120
Al ₂ O ₃	9.9	7.8	34.0	3700 \pm 400	0.02	1.616 \pm 0.003	59.5 \pm 0.2	\approx 60

Spectroscopic results are presented in Table I, and the experimental gas spectrum from the most potent material (the zirconia with 115 nm pores) is shown in Fig. 3. Evaluation is based on a fit using the expression $(a_0 + a_1\nu) \times \exp(-Sg(\nu, \Gamma)L)$, where ν denotes relative optical frequency, a_i , L and Γ are free fit parameters ($a_0 + a_1\nu$ accounts for the linear baseline caused by diode laser tuning), S the integrated absorption, and $g(\nu, \Gamma)$ the Lorentzian distribution. It should be noted that the fitted path length L represents an effective (Beer-Lambert weighted) average over the broad distribution of path lengths traveled by the light reaching the detector [33]. The moderate absorption renders L close to the actual average path length. The path length enhancement ($N = L/s$) of this zirconia is impressive, and corresponds to 750 passes through a conventional multipass cell of the same size. It is, however, important not to look only at the achieved path length enhancement. Besides being linearly proportional to μ'_s , the average path length of light transmitted through a turbid material is also proportional to the

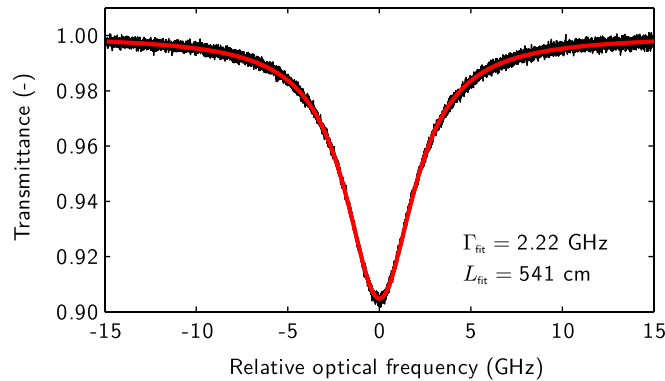


FIG. 3 (color online). Oxygen (O₂) absorption for light transmitted through the $s = 7.2$ mm thick zirconia material with 115 nm pores. The baseline-corrected experimental gas spectrum (black, noisy) is shown together with a fitted Lorentzian line shape (red, smooth). Fitted path length through gas is $L = 5.4$ m, i.e., $N = L/s = 750$ times the sample thickness. The fitted line HWHM is $\Gamma = 2.2$ GHz. The acquisition time was 10 s, and the detected power was about 10 nW (0.003% transmission).

square of the thickness [26]. In diffusive porous media, this holds also for the effective path length through gas [33], $L \propto s^2$, and the path length enhancement is therefore proportional to the material thickness, $N \propto s$. The suitability of a porous material as a random multipass gas cell is thus jointly determined by the scattering efficiency, the absorption of the solid, and the material porosity. Strong scattering and high porosity are ideal properties for this purpose, while absorption is detrimental both in terms of path length through gas and total transmission. Although the titania material exhibits the strongest scattering, the rather strong absorption at 760 nm makes it a less successful gas cell candidate than the zirconia (at this wavelength). It is also important to realize that losses due to scattering and absorption sets a limit to the maximum possible thickness. Diffuse light propagation causes transmitted intensity to decrease with $1/(s\mu'_s)$ [34], even if the absorption would be zero. For example, only 0.003% of the light incident on the 7.2 mm thick zirconia reached the detector. For comparison, the strong scattering combined with absorption of the titania (at 760 nm), makes it difficult to boost the path length through gas by increasing sample thickness (only 0.001% reaches through the 1.4 mm sample).

Another interesting aspect of the results in Table I is the observed linewidths. The linewidth of oxygen within the macroporous alumina agrees well with the width expected for oxygen at atmospheric pressure, i.e., 1.6 GHz. In great contrast, oxygen confined in the nanoporous materials exhibits significantly broadened absorption lines. This effect was only recently described [23,35], and is related to the fact that wall collisions no longer are negligible. For oxygen at ambient conditions, the mean free path between intermolecular collisions is about 60 nm. Since these collisions are the dominating source of line broadening at atmospheric conditions, it is not surprising that confinement in nanocavities gives rise to additional collisional broadening. Furthermore, the clear negative correlation between pore size and line broadening clearly shows the potential of wall collision broadening as means to measure pore size, as suggested in Ref. [23]. A related approach to pore size assessment was recently presented in connection to laser spectroscopy of Dicke narrowed lines of positronium confined in 5 nm cavities of porous silica [36].

While the above presented data are obtained for spectroscopy at 760 nm, similar results can be reached for a wide spectral range. The absorption of the ceramic materials is fairly low up to 4 μm , and by accompanying a longer wavelength with a scaling of pore size and sample thickness, the scattering efficiency and path length enhancement can be maintained. This means that porous ceramics may be used as spectroscopic gas cells for numerous important gases and vapors, including methane (CH_4), carbon dioxide (CO_2), carbon monoxide (CO), nitrous oxide (NO), nitrogen dioxide (NO_2), ammonia (NH_3) and water (H_2O) as well as atomic vapors such as Cs and Rb. An issue that requires further investigation is, however, how the response time of porous gas cells varies between gases, as well with pore size and cell geometry. While relatively inert gases, such as oxygen, have been found to move rapidly in and out of nanoporous alumina [23,35], the exchange of water vapor (known to be a “sticky” gas) is fairly slow [35].

To conclude, we have investigated light-gas interaction in strongly scattering porous media and have shown that such materials efficiently can function as miniature gas cells. Prominent absorption imprints as such may prove useful in fundamental studies of light propagation, but the phenomenon also have clear sensing applications. Important advantages of the porous gas cells described are their small size, the small gas volume needed ($< 1 \text{ cm}^3$), and their alignment-free nature. The most obvious disadvantage is that strong scattering results in only a small fraction of incident light reaching the detector. In the case of laser spectroscopy, another problem is speckle interference noise [32,35]. However, the topic of porous gas cells is new and significant improvements regarding detection schemes and gas cell design can be anticipated. For example, the pore structure can be optimized to yield stronger scattering [37], allowing smaller gas cells while maintaining or increasing L .

This work was funded by the Swedish Research Council. The authors gratefully acknowledge Erik Alerstam for assistance in PTOFS experiments, as well as Dmitry Khoptyar and Stefan Andersson-Engels for general collaboration on PTOFS.

*svensson@lens.unifi.it

Current address: European Laboratory for Non-Linear Spectroscopy (LENS), University of Florence, Italy.

- [1] D. S. Wiersma, P. Bartolini, A. Lagendijk, and R. Righini, *Nature (London)* **390**, 671 (1997).
- [2] M. Störzer, P. Gross, C. M. Aegerter, and G. Maret, *Phys. Rev. Lett.* **96**, 063904 (2006).
- [3] H. Cao, Y. G. Zhao, S. T. Ho, E. W. Seelig, Q. H. Wang, and R. P. H. Chang, *Phys. Rev. Lett.* **82**, 2278 (1999).
- [4] D. S. Wiersma, *Nature Phys.* **4**, 359 (2008).
- [5] O. L. Muskens, J. G. Rivas, R. E. Algra, E. P. A. M. Bakkers, and A. Lagendijk, *Nano Lett.* **8**, 2638 (2008).
- [6] I. Vellekoop, A. Lagendijk, and A. P. Mosk, *Nat. Photon.* **4**, 320 (2010).
- [7] J. White, *J. Opt. Soc. Am.* **32**, 285 (1942).
- [8] D. Herriott, R. Kompfner, and H. Kogelnik, *Appl. Opt.* **3**, 523 (1964).
- [9] A. O’Keefe and D. A. G. Deacon, *Rev. Sci. Instrum.* **59**, 2544 (1988).
- [10] R. Engeln, G. Berden, R. Peeters, and G. Meijer, *Rev. Sci. Instrum.* **69**, 3763 (1998).
- [11] J. Ye, L. S. Ma, and J. L. Hall, *J. Opt. Soc. Am. B* **15**, 6 (1998).
- [12] B. Bernhardt *et al.*, *Nat. Photon.* **4**, 55 (2009).
- [13] T. Ritari *et al.*, *Opt. Express* **12**, 4080 (2004).
- [14] S. Ghosh, J. E. Sharping, D. G. Ouzounov, and A. L. Gaeta, *Phys. Rev. Lett.* **94**, 093902 (2005).
- [15] Y. L. Hoo, S. J. Liu, H. L. Ho, and W. Jin, *IEEE Photonics Technol. Lett.* **22**, 296 (2010).
- [16] S. Tranchart, I. Bachir, and J. Destombes, *Appl. Opt.* **35**, 7070 (1996).
- [17] D. Masiyano, J. Hodgkinson, and R. Tatam, *Appl. Phys. B* **100**, 303 (2010).
- [18] J. Chen, A. Hangauer, R. Strzoda, and M.-C. Amann, *Appl. Phys. B* **100**, 417 (2010).
- [19] D. Qu, Z. Liu, and C. Gmachl, *Appl. Phys. Lett.* **93**, 014101 (2008).
- [20] J. Chen, A. Hangauer, R. Strzoda, M. Fleischer, and M.-C. Amann, *Opt. Lett.* **35**, 3577 (2010).
- [21] D. Das and A. Wilson, *Appl. Phys. B* **103**, 749 (2010).
- [22] M. Sjöholm, G. Somesfalean, J. Alnis, S. Andersson-Engels, and S. Svanberg, *Opt. Lett.* **26**, 16 (2001).
- [23] T. Svensson and Z. Shen, *Appl. Phys. Lett.* **96**, 021107 (2010).
- [24] J. Rouquerol *et al.*, *Pure Appl. Chem.* **66**, 1739 (1994).
- [25] T. Svensson, E. Alerstam, D. Khoptyar, J. Johansson, S. Folestad, and S. Andersson-Engels, *Rev. Sci. Instrum.* **80**, 063105 (2009).
- [26] D. Contini, F. Martelli, and G. Zaccanti, *Appl. Opt.* **36**, 4587 (1997).
- [27] A. Lagendijk and B. A. van Tiggelen, *Phys. Rep.* **270**, 143 (1996).
- [28] F. J. P. Schuurmans, D. Vanmaekelbergh, J. van de Lagemaat, and A. Lagendijk, *Science* **284**, 141 (1999).
- [29] S. Faez, P. M. Johnson, and A. Lagendijk, *Phys. Rev. Lett.* **103**, 053903 (2009).
- [30] T. Svensson, E. Alerstam, J. Johansson, and S. Andersson-Engels, *Opt. Lett.* **35**, 1740 (2010).
- [31] T. Svensson *et al.*, *Appl. Phys. B* **90**, 345 (2008).
- [32] T. Svensson, M. Andersson, L. Rippe, J. Johansson, S. Folestad, and S. Andersson-Engels, *Opt. Lett.* **33**, 80 (2008).
- [33] G. Somesfalean *et al.*, *Appl. Opt.* **41**, 3538 (2002).
- [34] M. C. W. van Rossum and T. M. Nieuwenhuizen, *Rev. Mod. Phys.* **71**, 313 (1999).
- [35] T. Svensson, M. Lewander, and S. Svanberg, *Opt. Express* **18**, 16460 (2010).
- [36] D. B. Cassidy, M. W. J. Bromley, L. C. Cota, T. H. Hisakado, H. W. K. Tom, and A. P. Mills, *Phys. Rev. Lett.* **106**, 023401 (2011).
- [37] J. G. Rivas, A. Lagendijk, R. W. Tjerkstra, D. Vanmaekelbergh, and J. J. Kelly, *Appl. Phys. Lett.* **80**, 4498 (2002).